

Voltage-Controlled and Current-Controlled Low Voltage STATCOM: A Comparison

L. Ribeiro¹, D. Simonetti¹

¹ Department of Electrical Engineering
 Power Electronics and Drives Laboratory, Federal University of Espírito Santo
 Campus of Goiabeiras, Vitória (Brazil)

Phone/Fax number: +55 27 4009-2644, e-mail: laila.sindra@gmail.com, d.simonetti@ele.ufes.br

Abstract. Inverter-based converters interconnecting DC-microgrids and AC-microgrids/grids are in a strong expansion. Besides power exchange, the inverter can be requested to furnish ancillary services and, among them, power factor compensation. This work presents a comparison between voltage control and current control in a low voltage inverter in a STATCOM operation. Both strategies use P&O controllers to control power factor, but in voltage-control the P&O adjust modulation index while in current-control P&O adjusts the current reference. HIL simulations show that both controllers can efficiently increase power factor; however, voltage control requires additional overcurrent protection. Current control can easily limit the devices current, but requires an extra current measurement when compared to the voltage controller, therefore has increased cost.

Key words. STATCOM, multilevel inverter, PLL, LCL filter, Hardware in the loop.

1. Introduction

Inverter-based converters interconnecting DC-microgrids and AC-microgrids/grids are in a strong expansion as renewable electrical resources are more and more tied to the electrical system, mainly due to the increase in energy demand as well as climate concerns. Rated power of such power sources, mainly wind and solar, ranges from a few kW to MW.

Also, interconnections at low-and-medium voltage distribution systems are increasing worldwide. As an example, from 2017 (end) to 2021 (end), residential solar farms in Brazil (below 75 kW) have jumped from 16,967 units to 614,680 units, leading to 3.8 GW of installed power [1].

It is expected that, in a near future, the total power furnished by prosumers below 75 kW will participate significantly in the power offer. It will be necessary to incorporate them, as a single unit or in a virtual power plant configuration, in the power system rules.

Along with the expansion of photovoltaic installations, DC microgrids are gaining increased interest, predicting the materialization of hybrid microgrids or DC/AC power system (Fig. 1).

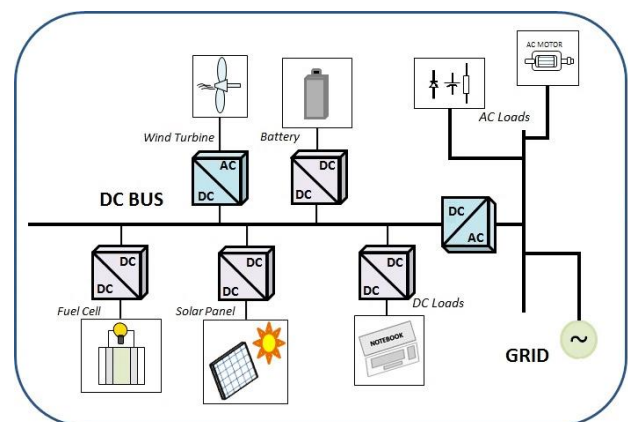


Fig.1. A basic AC/DC power system or hybrid microgrid.

In an integrated DC-microgrid and AC grid, the DC-AC converter connecting both systems is by default bidirectional. In the moments that an active power exchange is not required, the inverter can be requested to furnish ancillary services. Among them, power factor compensation arises.

In an electrical system, the amount of reactive power flow is relevant to maintain system reliability and power quality. The reduction of reactive power flowing in the system diminishes utility losses (lines, transformers, circuit breakers) improve voltage regulation, and liberates system capacity to deliver active power. As majority of electrical consumers present inductive behaviour, capacitors are a widespread solution to solve the problem, supplying reactive power. Meanwhile, this solution presents some negative aspects, as capacitors are not able to consume reactive power, and produces electrical transients during connection.

One solution to solve these constraints is the use of continuous-controlled power electronic converters operating as a reactive element. Such device can be controlled to be seen by the utility as a variable capacitor or inductor, being continuously adjusted to achieve a high power factor. The device is so-called STACOM and, applied to distribution levels, D-STACOM (STATIC COMPensator connected to the distribution system).

According to [2], when a STATCOM includes the possibility of an active power source or DC storage such that the injected current may include active power, it is defined as a Static Synchronous Generator (SSG). Although the inverter topology employed in this work allows such definition (as SSG), since this work focuses on reactive power control, it will be addressed as STATCOM.

This paper analyses the operation of a five-level single-phase STATCOM, evaluating its performance when employing current control or voltage control. The following topics are contemplated in the paper: section 2 summarize the principle of the STATCOM operation as reactive compensator as well as the description of the system designed in this work; section 3 describe Hardware In the Loop (HIL) simulations details and also discuss the results obtained. The last section (section 4) presents the conclusions of the analysis.

2. Low-Voltage Single-Phase D-STATCOM

A simplified schematic of a STATCOM is shown in Fig. 2a. The grid is the constant AC voltage source, and the STATCOM is the adjustable AC voltage source, always in phase with the grid voltage. Connecting both, there is a series reactor of reactance X_{TIE} [3, 4]. Fig 2b shows the three possible situations: if the controlled AC voltage source is adjusted to reply the grid voltage (same rms value and phase), no current flows and the STATCOM is in idle mode. Reducing the rms value of the STATCOM voltage, applying KVL the current lags the voltage and the STATCOM operates as an inductor. On the other hand, increasing the rms STATCOM voltage, the current leads the voltage and the device seems to be a capacitor.

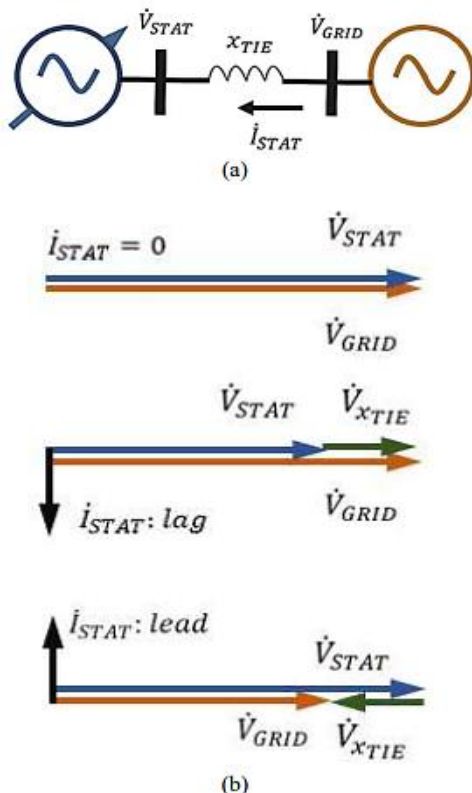


Fig.2. a) Simplified schematic of a STATCOM; b) The three operational conditions of a STATCOM.

The D-STATCOM considered in this work can be divided into 5 elements: DC supply, 5-level inverter, LCL filter, sensors and control. The device's main structure and its connection to the grid are presented in Fig. 3. The 5-level inverter is a full-bridge with T-cell first presented by [5]. One of the advantages of this topology is its capacity of producing 5-level using only 6 IGBT's, reducing cost and power losses. The inverter's topology is shown in Fig. 4. The use of multilevel converters even for low-voltage levels, as in a secondary distribution system, is being considering in some recent papers [6, 7].

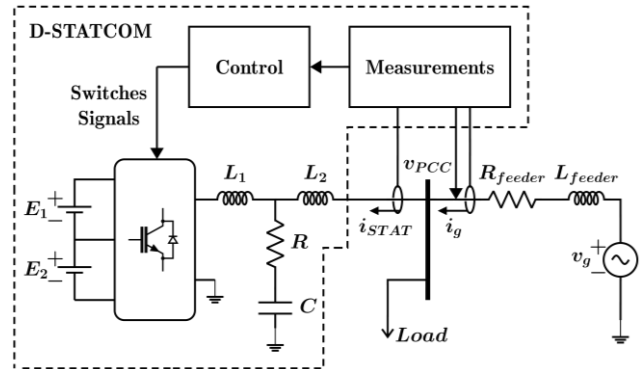


Fig.3. D-STATCOM main structure.

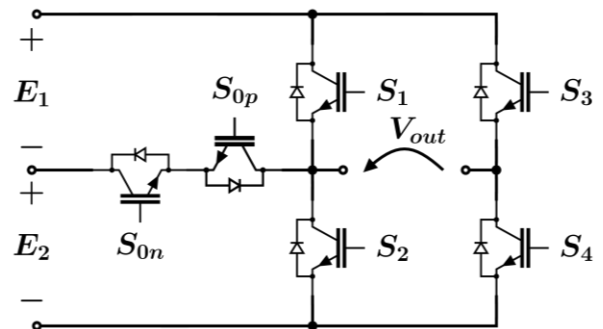


Fig.4. Full-bridge with T-cell topology.

Two strategies were evaluated to perform Power Factor (PF) control, and will be described in the subsections below, both using an adaptive Perturb and Observe (P&O) as controller. In PF-voltage control, the P&O adjust the modulation index (m), and therefore the amplitude, of the sinusoidal reference sent to a Pulse Width Modulator (PWM), while in PF-current control the P&O adjust the current reference sent to a current controller. In both strategies PF calculation employ Discrete Fourier Transform (DFT) to precisely calculate active and reactive power. According to experimental results [8], calculation of reactive power with other methods (such as $\alpha\beta$ or dq) can provide higher error. IEEE Std. 519 recommends that the measurement window of instruments employing DFT should be 12 cycles [9], therefore PF calculations and control actions are taken every 200ms (12 cycles in a 60Hz system). The Brazilian regulation is assumed in this paper, i.e., effective power factor must be 0.92 or above. In order to operate with a safe margin, the goal of the STATCOM is to keep power factor above 0.95 (inductive or capacitive, no restriction).

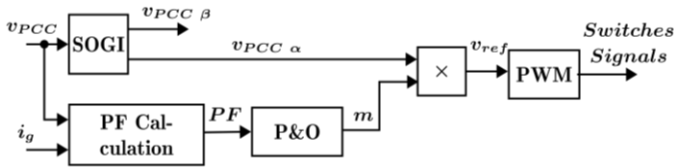


Fig.5. PF-voltage Control Block Diagram.

Table I. Summary of P&O algorithm for PF-voltage Controller.

Initialization:
$m = 0.9;$
$direction = 1;$
Main loop:
If PF decreased
$direction = -direction;$
If PF is below 0.95
$m = m + 0.1 \cdot direction \cdot (0.95 - PF);$

A. PF-Voltage Control Scheme

For PF-voltage control, only measurements of grid voltage and current at the Point of Common Coupling (PCC) (v_{PCC} and i_g) are required. The voltage measured is normalized and then becomes the input of a Second Order Generalized Integrator (SOGI) which provides a filtered signal, synchronized with v_{PCC} , to be used as voltage reference for the PWM. The PF-voltage control block diagram is presented in Fig. 5 and the algorithm implemented by P&O controller is summarized in Table I.

B. PF-Current Control Scheme

In addition to the measurements of PF-voltage control strategy, the PF-current control also requires the measurement of the current flowing through D-STATCOM (i_{STAT}). The block diagram of the proposed controller is shown in Fig. 6. Here, SOGI is used together

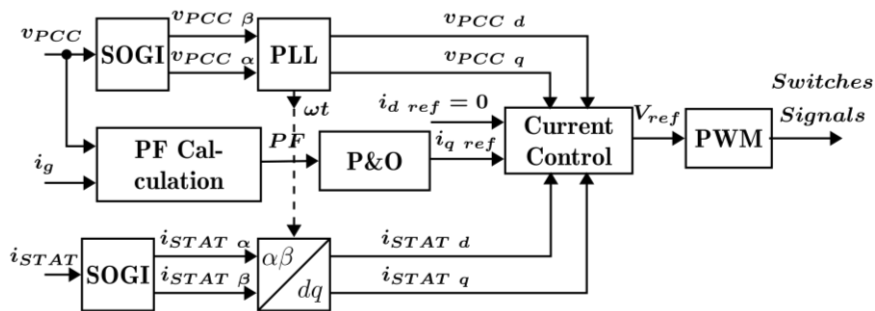


Fig.6. PF-Current Control Block Diagram.

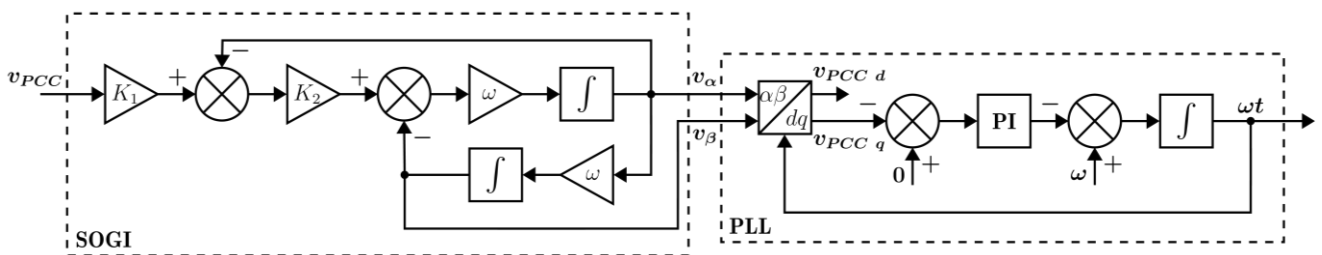


Fig.7. SOGI and PLL block diagram.

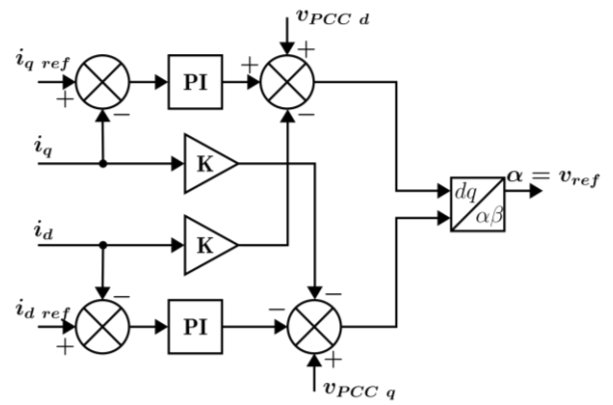


Fig.8. Current Control Block.

with a Phase-Locked Loop (PLL) (Fig. 7) to create a fictitious dq-frame. In this frame, a sine synchronized with v_{PCC} is mapped to a constant value in d-frame while a 90-degree lagged sine is mapped to a constant value in q-frame, therefore allowing controlling reactive power through the D-STATCOM by controlling the current in q-frame. The P&O controller is responsible for providing the q-current reference while the current controller in Fig. 8 provides the voltage reference sent to PWM. The P&O Current Controller logic is summarized in Table II.

Table II. Summary of P&O algorithm for PF-current Controller.

Initialization:
$i_{q\ ref} = 0;$
$direction = 1;$
Main loop:
If PF decreased
$direction = -direction;$
If PF is below 0.95
$i_{q\ ref} = i_{q\ ref} + 0.7 \cdot direction \cdot (0.95 - PF);$

3. HIL Simulation

In order to test the proposed controllers, Hardware In the Loop simulations were performed using Typhoon HIL 402 to emulate the power grid, D-STATCOM and loads while an eZdsp F28335 board implements control logic. Fig. 9 shows both eZdsp board and Typhoon HIL hardware. Since the equipment operate at different voltages, digital and analog signal conversions are performed.



Fig.9. Main hardware used in simulations.

Table III Simulation Parameters.

Description	Symbol	Value		
Power Grid				
Grid Frequency	f	60 Hz		
Grid Voltage	v_g	127 Vrms		
Feeder Resistance	R_{feeder}	0.0866 Ω		
Feeder Inductance	L_{feeder}	1.59e-4 H		
5-level Inverter				
Switching Frequency	f_{sw}	20.04 kHz		
DC Input	E_1, E_2	100 V		
Nominal Power	S_{nom}	4 kVA		
LCL Filter				
Inverter-side Inductance	L_1	5.281e-4 H		
Grid-side Inductance	L_2	2.109e-5 H		
Dampening Resistor	R	0.2617 Ω		
Filter Capacitance	C	3.289e-5 F		
Cut-off Frequency	f_c	6.162 kHz		
SOGI				
Normalization Gain	K_1	1/180 for voltage 1/44.5 for current		
SOGI Gain	K_2	1.414		
Nominal Frequency	ω	376.99 rad		
PLL				
Nominal Frequency	ω	376.99 rad		
Proportional Gain	K_p	376.99		
Integral Gain	K_i	13.16		
Current Controller				
Feedforward Gain	K	0.01555		
Proportional Gain	K_p	0.01		
Integral Gain	K_i	4		
Loads Tested				
Load Level	Load Types (PF)			Rectifier (Pout)
	R	RL	RC	
Light, 1kW	1	0.71	0.71	1kW
Medium, 5kW	1	0.8	0.8	5kW

The simulated system parameters are shown in Table III. To design LCL filter, the method proposed by [10] was employed. For SOGI and PLL parameters tuning, [11, 12] were consulted. Several types of loads were used in simulation, which are also described in Table III.

The following subsections presents a small portion of the results obtained during tests, highlighting the differences between the two studied control strategies.

A. PF-Voltage Results

The first test presented is a load change between light loads. System starts operating with Light R load and then load is changed to Light RC load at $t = 0s$. The results can be seen at Fig. 10. Since voltage changes are very slight, all voltage graphs are zoomed around peak voltages. The voltage controller reduces modulation index m in order to consume reactive power and keeps PF above limit. PF is corrected in less than 1 second after load change.

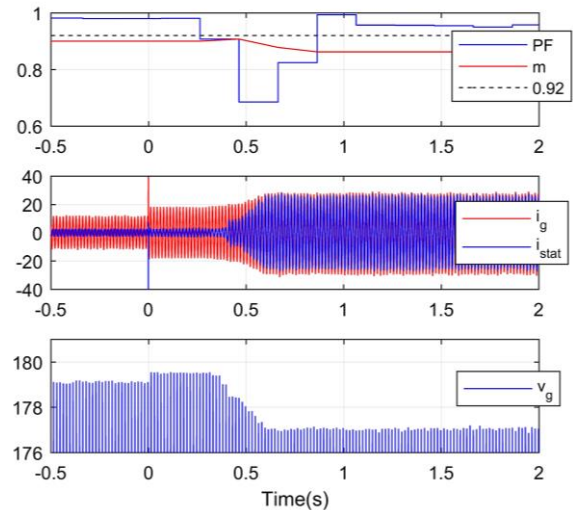


Fig.10. Light R to Light RC load change with PF-voltage controller.

In the next test shown here, a load change between heavy loads is performed. System starts operating with Heavy R load and then load is changed to Heavy Rectified load at $t = 0s$. Result is presented in Fig. 11. Here, the rectified load behaves as a very light capacitive load, and since PF does not drop below 0.95, no control action is performed and m is kept at 0.9.

For the last test, system starts at Light R load and then load is changed to Heavy RL load. Results are in Fig. 12, however the system oscillates and takes about 5 seconds to settle. The whole behaviour of PF and m is presented in Fig. 13, and steady state currents are shown in Fig. 14. The devices nominal current has a peak of 44.5A and, as highlighted in Fig. 14, the current gets too high, reaching almost 79.6A. Operating in this condition can be risky for the device, and is not recommended, except if it is designed to support such overcurrent.

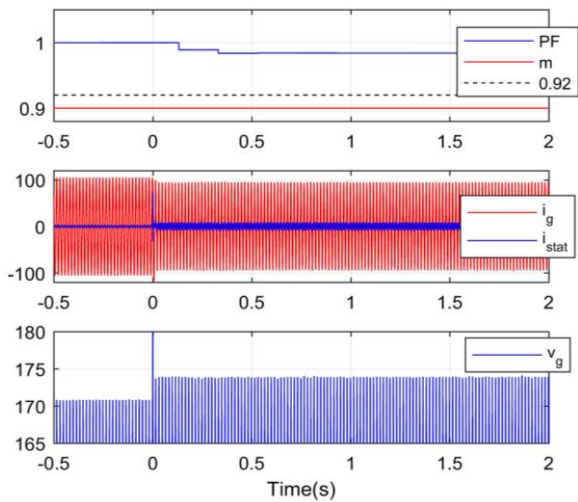


Fig.11. Heavy R to Heavy Rectified load change with PF-voltage controller.

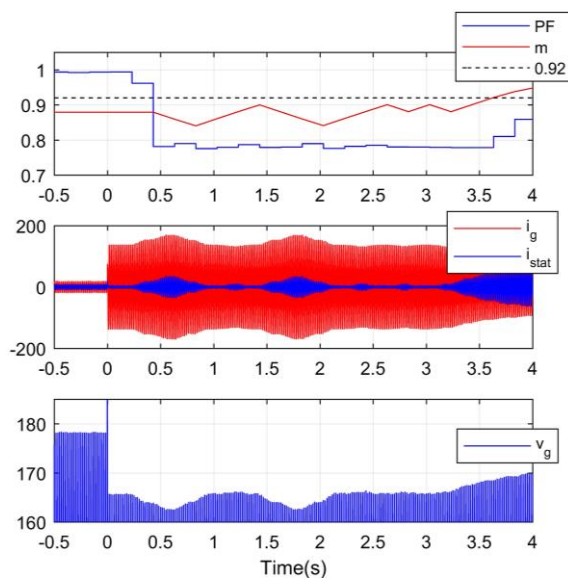


Fig.12. Light R to Heavy RL load change with PF-voltage controller.

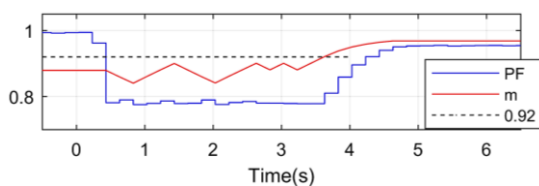


Fig.13. PF and m complete behaviour in Light R to Heavy RL load change with PF-voltage controller.

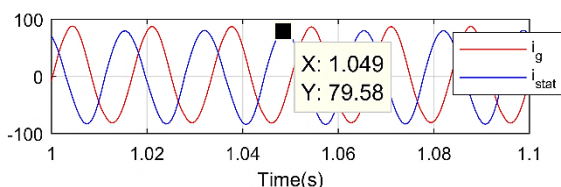


Fig.14. Grid and STATCOM currents with Heavy RL load and PF-voltage controller.

B. PF-Current Results

Same tests performed with PF-voltage controller will be performed with the current controlled version. Light R to

Light RC load change results is in Fig. 15. Here P&O controller reduces $i_{q\text{ ref}}$ (and therefore i_q) to absorb reactive power delivered by RC load and, similarly to the previous controller, PF is corrected in less than 1 second.

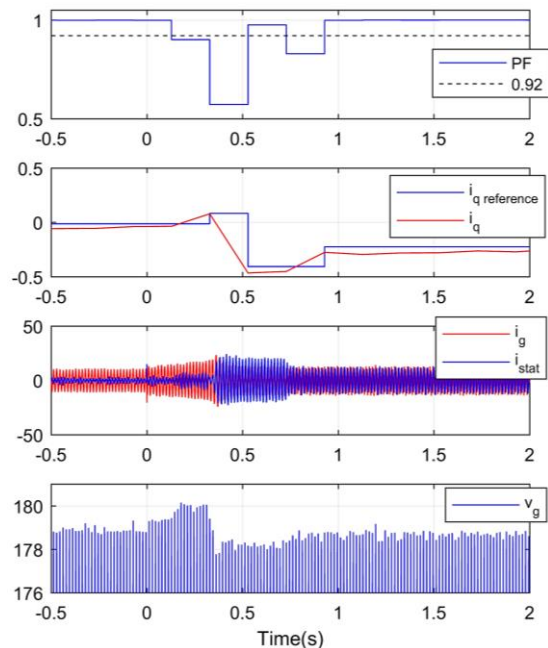


Fig.15. Light R to Light RC load change with PF-current controller.

The second test performed was Heavy R load to Heavy Rectified load, for which results are shown in Fig. 16. Behaviour was similar do PF-voltage case and no control action was necessary, since the Rectified load does not reduce PF below 0.95.

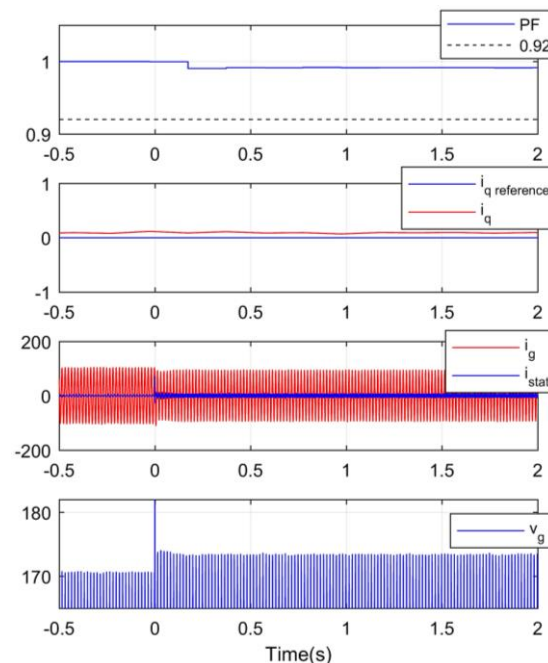


Fig.16. Heavy R to Heavy Rectified load change with PF-current controller.

The last result is for Light R load to Heavy RL load change, which results are presented in Fig. 17. Here, a key difference between voltage and current controllers stands out: current control allows to easily defining current limits and keep devices current below nominal value, therefore current stays controlled, allowing a safer

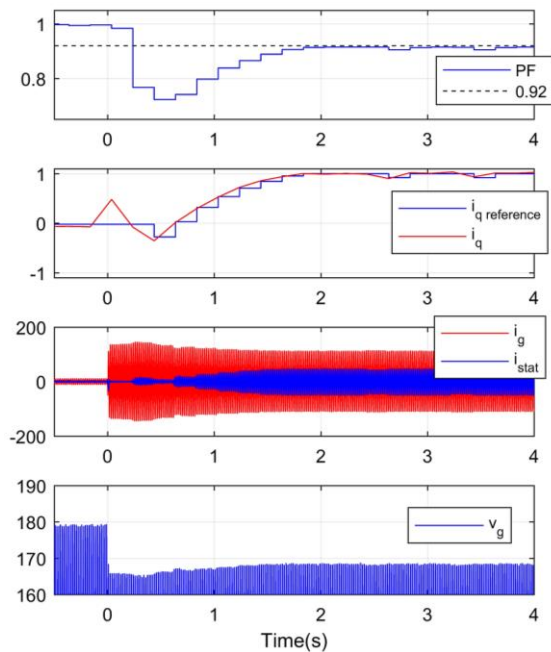


Fig.17. Light R to Heavy RL load change with PF-current controller.

operation of the inverter. As a drawback, PF is slightly below the desired value, but inverter can keep operating safely delivering reactive power at its maximum capacity. System reaches steady state in about 2 seconds, faster than the voltage-controlled system.

4. Conclusions

This work presents a comparison between voltage control and current control in a low voltage STATCOM. Both strategies use P&O controllers to control power factor, but in voltage-control the P&O adjust modulation index while in current-control P&O adjusts the current reference. In voltage control only measurements of PCC voltage and grid current are required, meanwhile current control requires also the D-STATCOM current measurement, therefore increasing its cost.

HIL simulations were performed to evaluate the controller's performance and they show that both can efficiently increase PF. However, voltage controller can reach currents above nominal value while operating, therefore need additional protection to avoid damages. In current controller is easy to implement current limitations, allowing the D-STATCOM to deliver or absorb the rated power without additional concerns.

Acknowledgements

This research is partially supported by Fundação de Amparo à Pesquisa e Inovação do Espírito Santo (FAPES). Authors also thank to Typhoon HIL Inc.

References

- [1] ANEEL, 2022. List of Distributed Generation Units (in Portuguese). Accessed in March, 19th, 2022. URL: <<https://app.powerbi.com/view?r=eyJrIjoiZjM4NjM0OWYtN2IwZS00YjViLTl1MjItN2E5MzBkN2ZlMzVkIiwidCI6IjQwZDZmOWI4LWVjYTctNDZhMi05MmQ0LWVhNGU5YzAxNzBIMSIsImMiOiR9>>.
- [2] N. G. Hingorani and L. Gyugyi, Understanding FACTS: concepts and technology of flexible AC transmission systems, IEEE, New York (1999).
- [3] J. Dixon, L. Moran, J. Rodriguez and R. Domke, "Reactive Power Compensation Technologies: State-of-the-Art Review," in Proceedings of the IEEE, vol. 93, no. 12, pp. 2144-2164, Dec. 2005.
- [4] C. A. C. Cavaliere, E. H. Watanabe, M. Aredes, P. G. Barbosa, F. D. Jesus, J. R. Carvalho, A. C. C. Moreira, F. E. R. Fraga, M. J. Leal. "Application of Statcom at distribution level: voltage regulation and power factor control", in portuguese (Aplicação do statcom na distribuição: Regulação de tensão e controle de fator de potência". V SBQEE (Seminário Brasileiro sobre Qualidade de Energia Elétrica), 2003, p.1-5.
- [5] P. K. Hinga, T. Ohnishi and T. Suzuki, "A new PWM inverter for photovoltaic power generation system," Proceedings of 1994 Power Electronics Specialist Conference - PESC'94, Taipei, Taiwan, 1994, pp. 391-395 vol.1.
- [6] S. De, D. Banerjee, K. Gopakumar, R. Ramchand and C. Patel, "Multilevel inverters for low-power application", IET Power Electronics, 4(4), 384-392.
- [7] D. S. L. Simonetti and X. Yuan. "Center-Tapped π -Type Single-Phase Cell". In: Brazilian Power Electronics Conference, 15.; Ieee Southern Power Electronics Conference, 5., 2019, Santos, Brazil. Proceedings. IEEE, Dec. 2019. p. 1-6.
- [8] A. d. J. C. Leal, C. L. T. Rodríguez and F. Santamaria, "Comparative of Power Calculation Methods for Single-Phase Systems under Sinusoidal and Non-Sinusoidal Operation," in Energies, vol. 13, no. 17, 4322, Aug. 2020.
- [9] IEEE, Std. 519 IEEE Recommended practice and requirements for harmonic control in electric power systems, IEEE, New York (2014).
- [10] A. Reznik, M. G. Simões, A. Al-Durra and S. M. Muyeen, "LCL Filter Design and Performance Analysis for Grid-Interconnected Systems," in IEEE Transactions on Industry Applications, vol. 50, no. 2, pp. 1225-1232, March-April 2014.
- [11] A. Kulkarni and V. John, "A novel design method for SOGI-PLL for minimum settling time and low unit vector distortion," IECON 2013 - 39th Annual Conference of the IEEE Industrial Electronics Society, 2013, pp. 274-279, doi: 10.1109/IECON.2013.6699148.
- [12] A. Kulkarni and V. John, "Analysis of Bandwidth-Unit-Vector-Distortion Tradeoff in PLL During Abnormal Grid Conditions," in IEEE Transactions on Industrial Electronics, vol. 60, no. 12, pp. 5820-5829, Dec. 2013, doi: 10.1109/TIE.2012.2236998.